JOURNAL

OF THE AMERICAN CHEMICAL SOCIETY

VOLUME 109, NUMBER 25 DECEMBER 9, 1987

Photodissociation Spectroscopy of the Negative Ion Dimer of Toluquinone

Paul B. Comita and John I. Brauman*

Contribution from the Department of Chemistry, Stanford University, Stanford, California 94305. *Received October 20, 1986*

Abstract: The photodissociation spectrum of the negative ion dimer of toluquinone has been determined in an ion cyclotron resonance spectrometer. A charge resonance transition at 1.9 eV, which displays individual vibronic transitions at high resolution, has been identified. The bond dissociation energy and electron affinity of the dimer were determined from the data. The charge resonance transition was fit to a single-oscillator theoretical model and details of the electronic structure were extracted. The fit to the data indicates that the odd electron in the radical ion dimer is strongly localized.

The nature of the bonding between the constituents of molecular ionic clusters has not yet been well-defined, due to the relatively little thermodynamic and spectroscopic information available on these species. Molecular ion dimers, the simplest of the clusters, can be taken as a starting point for investigations into the bonding between molecular ions and their corresponding neutrals. We have obtained spectroscopic data for the first time on a negative ion dimer of a quinone via gas-phase photodissociation spectroscopy. The data contain energetic information that has been theoretically analyzed and may help to elucidate the electronic structure of a species which can either be described as a radical ion complexed to a neutral molecule in the localized limit or a species with strong electronic coupling between the subunits in the ground state in the delocalized limit.

Positively or negatively charged radical ion dimers, such as the quinone negative ion dimer, are formally analogous to inorganic mixed valence complexes, which have been well-studied in condensed media and may be expected to exhibit optical charge transfer transitions. In the gas phase, many studies have been undertaken recently on molecular positive ion dimers. For example, the photodissociation dynamics of small cation dimers including $(SO_2)_2^+$, $(N_2)_2^+$, $(CO_2)_2^+$, and $(NO)_2^+$ have been studied with crossed ion beam and laser beam techniques,[1] providing information on product energy distributions and excited states involved in the photodissociation process. Aromatic and olefinic radical cation dimers have been studied both in matrices and in the gas phase. The early matrix work has been useful in determining spectroscopic properties of dimer cations.[2] Vibronic structure has been reported in the photodissociation spectrum of $(CO)_2^+$, although the vibronic structure was not analyzed in detail.[3] Gas-phase thermodynamic data have been obtained for ethylene cluster ions[4] and benzene cation dimers.[5] These studies have been useful in interpreting the nature of the bonding between radical ions and their corresponding neutrals.

At present, much less is known about the spectroscopic and thermodynamic properties of negative molecular ion dimers. Dinegative ion dimers in solution or in the solid state have been studied by a number of different research groups.[6] In contrast, reports of the generation of mononegative radical ion dimers in either the gas phase or a matrix are rare. The spectroscopic properties of anthracene dimer anion have been studied in a matrix.[7] This radical anion has been found to be unstable both thermally and optically. In the gas phase, three different methods have been used to generate negative ion dimers. Electron attachment to CO_2 clusters generated $(CO_2)_2^-$ in a time-of-flight mass spectrometer.[8] Negative ion dimers of nitrobenzenes have been generated with use of a high-pressure chemical ionization source.[9] Collisional charge transfer from alkali atoms to molecular clusters of Cl_2 and SO_2 has been used[10] to generate $(Cl_2)_2^-$ and $(SO_2)_2^-$. Some thermodynamic information, but virtually no spectroscopic information, on these gas-phase clusters has been obtained. One report has appeared recently describing the photoelectron spectrum of the O_4^- cluster ion in a pulsed photoelectron spectrometer.[11] In an effort to understand better the spectroscopic

(1) Jarrold, M. F.; Illies, A. J.; Bowers, M. T. *J. Chem. Phys.* **1985**, *82*, 1832; **1984**, *81*, 214; **1983**, *79*, 6086. Illies, A. J.; Jarrold, M. F.; Wagner-Redeker, W.; Bowers, M. T. *J. Phys. Chem.* **1984**, *88*, 5204.

(2) Badger, B.; Brocklehurst, B. *Trans. Faraday Soc.* **1969**, *65*, 2582; **1969**, *65*, 2588, 2576; **1970**, *66*, 2939. Buhler, R. E.; Funk, W. *J. Phys. Chem.* **1975**, *79*, 2098. Kira, A.; Imamura, M.; Shida, T. *J. Phys. Chem.* **1976**, *80*, 1445.

(3) Ostrander, S. C.; Sanders, L.; Weissharr, J. C. *J. Chem. Phys.* **1986**, *84*, 529.

(4) Bowers, M. T.; Elleman, D. D.; Beauchamp, J. L. *J. Phys. Chem.* **1968**, *72*, 3599. Ceyer, S. T.; Tiedemann, P. W.; Ng, C.; Mahan, B. H.; Lee, Y. T. *J. Chem. Phys.* **1979**, *70*, 2138.

(5) Meot-Ner, M.; Hamlet, P.; Hunter, E. P.; Field, F. H. *J. Am. Chem. Soc.* **1978**, *100*, 5466. Meot-Ner, M. *J. Phys. Chem.* **1980**, *84*, 2724.

(6) For leading references see: Bozio, R.; Girlando, A.; Pecile, C. *Chem. Phys.* **1977**, *21*, 257. Bieber, A.; Andre, J. *Ibid.* **1974**, *5*, 166.

(7) Shida, T.; Iwata, S. *J. Chem. Phys.* **1972**, *56*, 2858.

(8) Klots, C. E.; Compton, R. N. *J. Chem. Phys.* **1977**, *67*, 1779.

(9) Burinsky, D. J.; Fukuda, E. K.; Campana, J. E. *J. Am. Chem. Soc.* **1984**, *106*, 2770.

(10) Bowen, K. H.; Liesegang, G. H.; Sanders, R. A.; Herschbach, D. R. *J. Phys. Chem.* **1983**, *87*, 557.

(11) Posey, L. A.; Deluca, M. J.; Johnson, M. A. *Chem. Phys. Lett.* **1986**, *131*, 170.

0002-7863/87/1509-7591$01.50/0

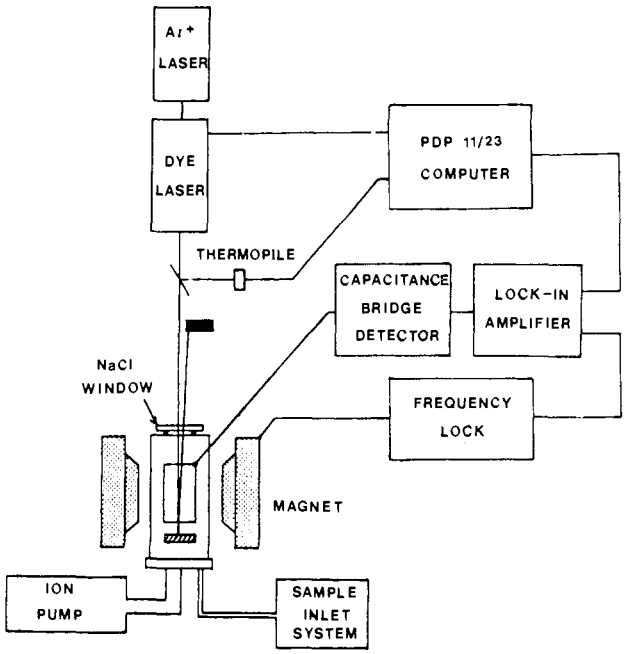

Figure 1. Schematic diagram of the experimental apparatus.

and thermodynamic properties of negative ion dimers, we have undertaken an investigation of a quinone radical ion dimer, specifically the dimer of toluquinone $(TQ)_2^-$. This cluster ion has been generated in an ion cyclotron resonance spectrometer and studied with use of photodissociation spectroscopy. An excited state of the dimer has been observed at low energies (1.9 eV) and is assigned to a charge resonance transition. At high resolution, vibronic structure which appears as resonances in the photodissociation cross section can be resolved. Upper and lower limits to the bond dissociation energy have been determined from an analysis of the photodissociation spectrum. The bond dissociation energy, in conjunction with the electron affinity of the monomer quinone, is used to determine the electron affinity of the dimer. The charge resonance transition has been calculated and fit to the observed spectrum with use of the single-oscillator vibronic-coupling model of Piepho, Krausz, and Schatz. The comparison of this theory with a detailed moderate resolution (1 cm^{-1}) spectrum has yielded some information on the applicability of this model to transitions in molecular ions.

Experimental Section

Ion generation and trapping were accomplished by using an ion cyclotron resonance spectrometer (ICR) operated in a drift configuration. Details of this apparatus have been described previously.[12,13] A schematic diagram of the experimental apparatus is shown in Figure 1. In general, ions are generated in the source region of the cell and drift into the analyzer region due to an electric field set up by the source plate voltages. The ions are detected in the analyzer region with the use of a capacitance bridge detector operated continuously. The radio frequency used to excite ion motion is supplied by a lock-in amplifier (PAR 124A). Due to the narrow line widths (1-3 G) achieved with this instrument, small frequency shifts in the ion resonance frequency are experienced when photodecreases occur, making measurements of a fractional signal decrease difficult. These difficulties have been overcome with the implementation of a frequency lock system, incorporating a second lock-in amplifier (PAR HR-8) which modulates the magnetic field through an amplified reference frequency applied to a pair of Helmholz coils.

The light source for rapid-scan, low-resolution experiments was a 1000 W arc lamp used with a $^1/_4$-m high-intensity grating monochromator (Schoeffel Instrument Corp. GM 250). Visible and UV gratings used in conjunction with matched pairs of slits gave spectral bandwidths of 5 to 24 nm fwhm. The higher resolution light source consisted of a dye laser (Coherent Radiation CR-590) pumped by an argon ion laser (Coherent Radiation CR-12) or a krypton ion laser (Spectra-Physics Model 171). The dyes used were Rhodamine 6G, DCM, LDS 698, LD 700, LDS 751, LDS 820, HITC, and DOTC. The maximum output power of the dye laser was in the 250–800 mW range. Approximately 4% of the output beam was split into a thermopile for measurement of the photon flux. The laser light was expanded with a beam expander to irradiate the entire volume of the cell. The output wavelength was selected by a birefringent filter in the laser cavity. This tuning element was rotated by a stepping motor controlled by a DEC MINC 11/23 computer. The dye laser spectral bandwidth with the tuning element is less than 1 cm^{-1}. Absolute calibration of the laser wavelength was accomplished with a Beck reversion spectroscope, which in turn was calibrated with a He-Ne laser. Absolute wavelengths are accurate to within 0.3 nm.

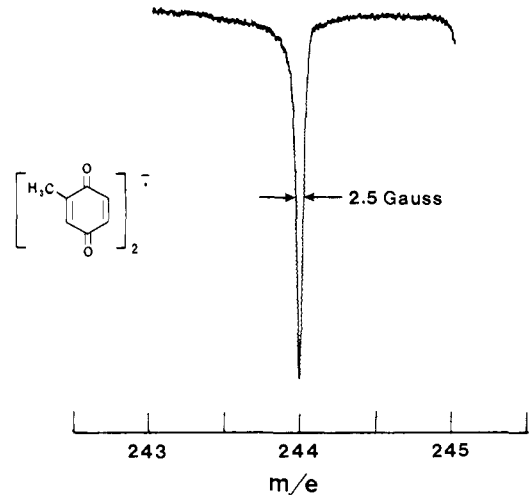

Figure 2. Line shape of the ICR signal of $(TQ)_2^-$.

The fractional signal decrease in the ion signal was obtained along with the photon flux at each wavelength. These data were acquired and stored on a DEC MINC 11/23 computer. When a large region of the spectrum was acquired it was necessary to overlap measurements from several different runs. The fractional signal decrease due to ion photodissociation was calculated by using a steady state model,[14] where the relative photodissociation cross section is given by the following expression:

$$\sigma(\lambda) \propto \frac{F(\lambda)}{\rho(\lambda)g[1 - F(\lambda)]} \quad (1)$$

In this equation, $F(\lambda)$ represents the fractional signal decrease, g is the geometrical overlap factor for the light beam and the ICR cell, and $\rho(\lambda)$ is the photon flux. The radical ion dimer of TQ was generated through dissociative electron impact on the corresponding neutral quinhydrone charge transfer complex

$$TQ^{\cdot}H_2TQ + e^- \rightarrow (TQ)_2^- + H_2 \quad (2)$$

The presence of NF_3 has been found to aid dimer generation and improves the stability of the ion signal considerably. Other buffer gases were not as effective as NF_3. Optimal pressures for dimer generation were in the 10^{-6} Torr range.

Results

For the present study, it was necessary to establish the molecular constitution of the dimer. Specifically, it was necessary to establish whether the hydrogens bonded to oxygen in the quinhydrone precursor are present in the dimer anion. Two experiments establish that they are not and that the dimer consists of two TQ monomers with an excess electron.

The first experiment consisted of labeling the precursor quinhydrone with 50% deuterium in the hydrogens bonded to oxygen. If these hydrogen atoms (or deuterium atoms) are present in the dimer anion, the dimer will show resonances at several different cyclotron frequencies depending upon the number of each isotope. Only one resonant frequency was observed, however, indicating neither of these hydrogen atoms (or deuterium atoms) are present in the dimer.

(12) Jackson, R. L.; Zimmerman, A. H.; Brauman, J. I. *J. Chem. Phys.* **1979**, *71*, 2088.
(13) Marks, J.; Drzaic, P. S.; Foster, R. F.; Wetzel, D. M.; Brauman, J. I.; Uppal, J. S.; Staley, R. S. *Rev. Sci. Instrum.* **1987**, *58*, 1460.
(14) Zimmerman, A. H. Ph.D. Thesis, Stanford University, 1977.

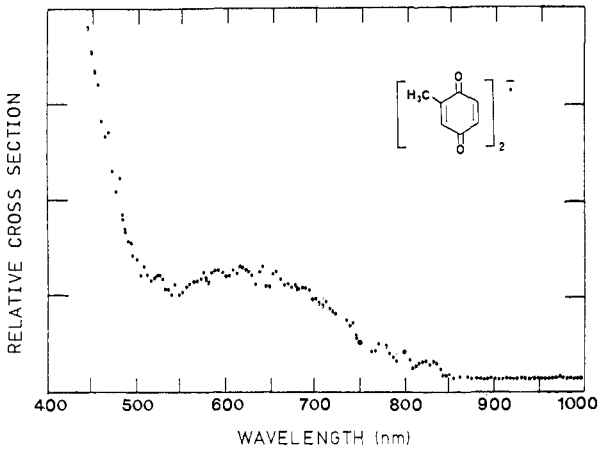

Figure 3. Low-resolution photodissociation spectrum of $(TQ)_2^-$.

The second method is an absolute mass measurement. The line width of the dimer ion signal under typical experimental conditions was 2.5 G (see Figure 2). This line width is more than sufficient to undertake high-resolution studies of ion mass. The equation for motion in an ion cyclotron spectrometer[15] is given by

$$\omega^2 = \left(\frac{qH}{m}\right)^2 - \frac{4qV}{md^2} \tag{3}$$

where ω is the cyclotron resonance frequency, q is the charge of the ion, m is the mass of the ion, H is the magnetic field strength, V is the trapping plate voltage, and d is the distance between trapping plates. Expanding this equation in a power series about ω and truncating the series after two terms yields (4) after manipulation.

$$\frac{m}{z} = H\left[\frac{1}{\omega} - \frac{1}{\omega_{ref}}\right] - \frac{2V}{d^2}\left[\frac{1}{\omega^2} - \frac{1}{(\omega_{ref})^2}\right] \tag{4}$$

Exact m/z can thus be determined with a known reference frequency ω_{ref}. The results of this determination for two different dimers, $(TQ)_2^-$ and $(TQ\text{–}PBQ)^-$, were 244.1 ± 0.4 and 230.2 ± 0.4 amu, respectively. The calculated molecular masses are 244.26 and 230.23 amu, respectively.

Photodissociation Studies. In the visible region of the spectrum, $(TQ)_2^-$ undergoes photodissociation to generate TQ^- and by inference TQ. A mass scan under conditions for a photodissociation experiment shows the presence of both the monomer TQ^- and the dimer $(TQ)_2^-$. The photodisappearance of $(TQ)_2^-$ is tracked by a photoappearance of TQ^- throughout the spectral range studied. The wavelength dependence of the photodissociation at low spectral resolution is displayed in Figure 3. Two striking features of the photodissociation spectrum can be noticed: the onset for photodissociation occurs at very low energy (~1.5 eV) and there is a broad resonance centered at 1.91 eV.

A low-resolution spectrum of electron photodetachment of PBQ^- is displayed in Figure 4. The onset for photodetachment is 1.99 eV (610–615 nm).[16] The onset for TQ^- is expected to be at 1.92 eV according to relative electron affinity data.[17]

In order to establish a threshold for photodissociation, a higher resolution (<1 cm^{-1}) study was undertaken in the region from 600 to 900 nm. These data are displayed in Figure 5. A sequence of vibronic transitions can be identified in this spectrum with a 460-cm^{-1} spacing. The relative photodissociation cross section slowly decreases to approximately zero at 900 nm.

Discussion

The wavelength dependence of the relative photodissociation cross section of the dimer anion reveals a broad resonance at 1.91 eV. A resonance at this low energy is not present in the monomer negative ion of PBQ or in the neutral PBQ. The electronic states of the monomer of PBQ should be little perturbed energetically by a methyl group, and PBQ is therefore expected to be a good model for TQ, which has been much less studied.

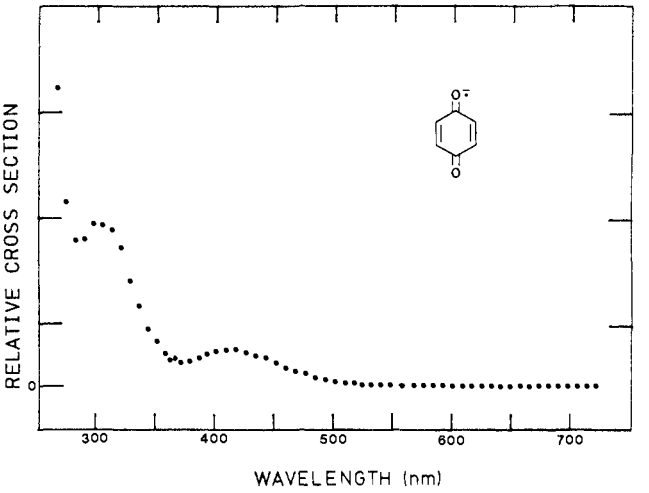

Figure 4. Low-resolution electron photodetachment spectrum of PBQ^-.

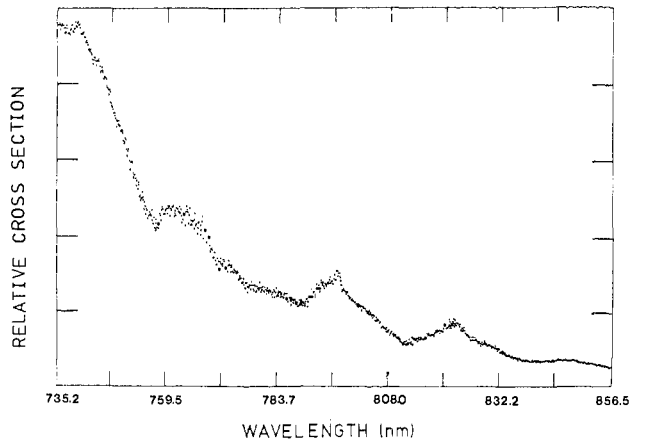

Figure 5. High-resolution (1 cm^{-1}) photodissociation spectrum of $(TQ)_2^-$ from 735 to 856 nm.

The photodetachment spectrum of PBQ^- contains resonances at 2.95 and 3.98 eV (Figure 4). Both of these transitions are close to those in solution[18] (2.88 and 3.93 eV) and in agreement with theory[19] (3.01 and 4.24 eV). Electron transmission studies of PBQ in the gas phase[20] also show negative ion states at 0.69 and 2.11 eV, which correspond to transitions of 2.68 and 4.1 eV using our experimentally determined electron affinity of 1.99 eV. Excitations for the neutral PBQ have been observed at 2.48, 4.07, and 5.13 eV.[21] These transitions correspond to singlet–singlet excitations, and the energies agree well with ab initio calculations.[22]

The observation of a resonance at 1.91 eV in the photodissociation spectrum of $(TQ)_2^-$ indicates a transition between a dimer ground state and dimer excited state. No excited states of the monomer ion or neutral are low enough in energy to account for this transition. The origin of a low-energy excited state in the dimer can be explained in terms of an interaction between neutral and anion states following McHale and Simons' treatment.[23] The

(15) Beauchamp, J. L.; Armstrong, J. T. *Rev. Sci. Instrum.* **1969**, *40*, 123.
(16) Marks, J.; Comita, P. B.; Brauman, J. I. *J. Am. Chem. Soc.* **1985**, *107*, 3718.
(17) Fukuda, E. K.; McIver, R. T. *J. Am. Chem. Soc.* **1985**, *107*, 2291.
(18) Fukuzumi, S.; Ono, Y.; Keii, T. *Bull. Chem. Soc. Jpn.* **1973**, *46*, 3353.
(19) Chang, H.; Jaffe, H.; Masmanidis, C. *J. Phys. Chem.* **1975**, *79*, 1118.
(20) Harada, Y. *Mol. Phys.* **1964**, *8*, 273.
(21) Modelli, A.; Burrow, P. *J. Phys. Chem.* **1984**, *88*, 3550. Cooper, C.; Naff, W.; Compton, R. *J. Chem. Phys.* **1975**, *63*, 2752. Goodman, J.; Brus, L. E. *J. Chem. Phys.* **1978**, *69*, 1604. Trommsdorf, H. P. *Ibid.* **1972**, *56*, 5358. Lafore, M. M.; Trommsdorf, H. P. *Ibid.* **1976**, *64*, 3791. Terhorst, G.; Kommandeur, J. *Chem. Phys.* **1979**, *44*, 287.
(22) Ha, T.-K. *Mol. Phys.* **1983**, *49*, 1471.
(23) McHale, J.; Simons, J. *J. Chem. Phys.* **1980**, *72*, 425.

absorption is assigned to a transition between symmetric and antisymmetric dimer anion wave functions from the ground state molecule (M) and anion (N) wave functions at sites A and B:

$$\Phi^{\pm} = \frac{1}{\sqrt{2}}(\Psi_N^A\Psi_M^B \pm \Psi_M^A\Psi_N^B) \quad (5)$$

The observation of this charge resonance transition via photodissociation indicates that the dissociation threshold is below the energy of the excited state. The behavior of the cross section with energy shows that the intensity of the transition decreases with decreasing energy. The intensities of the vibronic transitions are governed by the overlap of the vibronic wave functions of the ground and excited states. Resonances due to hot band transitions are expected to decrease in intensity due to the decreased population of the higher vibrational states in the ground electronic manifold. With the fraction of molecules in an individual vibronic state given by the Boltzmann equation, the integrated intensities of the vibronic transitions in the hot band region were found to fit best for a vibrational temperature of 300 K for the 460-cm^{-1} sequence. In the hot band region, the photodissociation cross section is proportional to the ground vibronic state population up to energies where the transitions result from the ground vibrational state to the excited state, at which point the intensities are primarily governed by Franck–Condon factors.[25] The resonance after which the intensity deviates from that due to ground-state populations is at 12158 cm^{-1} (1.5 eV) and can be assigned as the 0–0 vibronic transition within the framework of this simple Franck–Condon analysis. A more detailed analysis of the spectroscopic transitions which take into account the vibronic interaction of the two monomer subunits is described below. It will be seen that within this model, the Born–Oppenheimer assumption is inadequate, and it is not useful to speak of Franck–Condon transitions between two surfaces because of the strength of the vibronic interaction.

It remains useful, however, to probe the energies involved in the interaction between the molecule and ion with the values derived from the Franck–Condon analysis. With the assignment of the 0–0 transition and a value for the maximum of the charge resonance transition, an estimate of the distortion energy involved in the excitation from the ground to excited state can be made. The maximum of the band is between 1.99 and 1.91 eV. The distortion energy is thus 0.49 to 0.41 eV. The reasonableness of this value can be affirmed by two independent methods.[24,25]

With use of the results from a configuration interaction treatment of the ground and excited dimer states,[23] the charge resonance excitation energy is given by

$$\Delta E_{CR} = [(H_{BB} - H_{AA})^2 + 4(H_{AB})^2]^{1/2} \quad (6)$$

With zero overlap of wave functions on the neutral and anion sites, the H_{AA} matrix element is the sum of the ground-state equilibrium energies of an undistorted anion and molecule

$$\langle\Psi_g^{(0)}|H|\Psi_g^{(0)}\rangle \equiv H_{AA} = E^-(Q_N) + E^0(Q_M) \quad (7)$$

where E refers to energy, Q refers to geometry, superscript minus refers to anion, and superscript zero refers to the neutral. The H_{BB} matrix element is the sum of the energies of the distorted molecule and distorted anion

$$\langle\Psi_e^{(0)}|H|\Psi_e^{(0)}\rangle \equiv H_{BB} = E^-(Q_M) + E^0(Q_N) \quad (8)$$

The off-diagonal matrix element H_{AB} is simplified[21] to give

$$H_{AB} = \left\langle \Phi_B^L \middle| \frac{-1}{2}\nabla^2 + V_A^{eff} + V_B^{eff} \middle| \Phi_A^L \right\rangle \quad (9)$$

where V_i is the effective electron-neutral molecule potential at site i involving nuclear attraction and Coulomb and exchange interactions, and Φ_i^L is the LUMO at site i.

The resonance integral H_{AB} can be evaluated by using the experimental charge resonance energy and the experimental distortion energy δ determined by the previous assignment of the 0–0 vibronic transition

$$H_{AB} = [(\Delta E^2_{CR} - \delta^2)/4]^{1/2} = 0.93 \text{ eV} \quad (10)$$

This value can be regarded as a lower limit and a rough estimate of the bond dissociation energy of the dimer $(TQ)_2^-$. An approximate upper limit to the bond dissociation energy is given by the energy where the photodissociation cross section approaches zero. This is at approximately 1.38 eV (31.8 kcal/mol). With use of the 0.93 value as the best estimate to the bond dissociation energy of the dimer and a thermochemical cycle, the electron affinity of the dimer can be evaluated

$$\begin{aligned} EA_{(TQ_2)} &= BDE_{(TQ_2^-)} + EA_{(TQ_0)} - BDE_{(TQ_{2o})} \\ &= 0.93 \text{ eV} + 1.92 \text{ eV} - (0.17 \text{ eV}) = 2.7\text{eV} \end{aligned}$$

The binding energy of the electron is thus substantially increased in the dimer.

The bond dissociation energy of the negative ion dimer of TQ (21 kcal/mol) is similar to that of the positive ion dimers of the aromatic hydrocarbons (17–19 kcal/mol).[2-4] This is in accord with theoretical estimates which indicate that the bonding interactions of negative ion dimers are of the same order of magnitude as those of positive ion dimers.[26]

The criterion for delocalization has been defined without the inclusion of vibronic coupling by the formula

$$\delta/2H_{AB} \ll 1$$

The assigned 0–0 transition and the corresponding H_{AB}, values determined from the Franck–Condon analysis, can be used to arrive at a value of 0.25 for $\delta/2H_{AB}$. This corresponds to a *delocalized* system. The vibronic transitions would then be interpreted in terms of an excitation to a relaxed excited state. The extent of the upper state relaxation would be 7 $\hbar\omega c$ or approximately 0.45 eV, with the 0–0 transition at 1.5 eV.

Spectral Analysis of the Charge Resonance Transition

In this section, we fit the charge resonance in the photodissociation spectrum of $(TQ)_2^-$ to a model for intervalence transfer transitions developed by Piepho, Krausz, Schatz, and Wong.[27-30] This model is a vibronic coupling model and solves the intervalence transfer transition problem numerically with both electronic and vibronic coupling. The position and intensity of the individual vibronic transitions within the charge resonance band can be calculated to arbitrary accuracy by diagonalizing a truncated infinite tridiagonal matrix.

As is the case for other optical transitions of this general type, the question of which treatment is appropriate remains controversial,[31] and generally one cannot prove which model is correct by the quality of the fit. Nevertheless, the system appears to exhibit characteristics appropriate for the PKS analysis, and we proceed on that basis.

The utility of the PKS model derives from the formulas being applicable for either localized or delocalized systems. Since the

(24) The distortion energy for a collection of N harmonic oscillators perturbed by the electric field of an additional electron can be approximately calculated by using the nuclear Hamiltonian for a charged harmonic oscillator in a uniform electric field.[25] The total distortion energy is $N\delta = -q^2E|m\omega^2N$. This expression can be evaluated for $(TQ)_2^-$ with the use of an independently evaluated distortion energy of an analogous dimer anion.[23] Considering only the carbon–carbon bond framework, and using the assumption that the 50 normal modes in $(TQ)_2^-$ have the same average frequency, $N\delta = 0.32$ to 0.54 eV, in the same range as the experimental spectroscopic distortion energy.

(25) Cohen-Tannoudji, C.; Diu, B.; Laloe, F. *Quantum Mechanics*; Wiley and Sons: New York, 1977; Vol. 1, p 552.

(26) Badger, B.; Brocklehurst, B. *Trans. Faraday Soc.* **1970**, *66*, 2939. An alternative view is given by: Malar, E. J. P.; Chandra, A. K. *J. Phys. Chem.* **1981**, *85*, 2190.

(27) Piepho, S. B.; Krausz, E. R.; Schatz, P. N. *J. Am. Chem. Soc.* **1978**, *100*, 2996.

(28) Wong, K. Y.; Schatz, P. N.; Piepho, S. B. *J. Am. Chem. Soc.* **1979**, *101*, 2793.

(29) Wong, K. Y.; Schatz, P. N. *Prog. Inorg. Chem.* **1982**, *28*, 369-449.

(30) Wong, K. Y. *Inorg. Chem.* **1984**, *23*, 1285.

(31) Zhang, L.-T.; Ko, J.; Ondrechen, M. J. *J. Am. Chem. Soc.* **1987**, *109*, 1666. Ondrechen, M. J.; Ko, J.; Zhang, L.-T. *Ibid.* **1987**, *109*, 1672.

intensity maximum of the transition of $(TQ)_2^-$ is in the visible region of the spectrum, and not the near-IR, one might expect that this system is strongly coupled, either electronically or vibronically, and may therefore comprise in the former case a delocalized system. In this case, vibronic coupling, i.e., the vibrational and electronic excitations being coupled, must be taken into account, in order to model the transition accurately.

The model is a single harmonic oscillator model and takes advantage of the properties of harmonic oscillator functions. For this reason, it might appear too simple a model for a many-oscillator dimer such as $(TQ)_2^-$, but in fact the theory has modeled transitions in complex inorganic molecules reasonably well. In our application, however, the monomer subunit comprising $(PBQ)_2^-$ contains six totally symmetric normal coordinates, which are the active vibrations involved in the intervalence transition, for the case when the neutral and ion have the same point group symmetry.

A detailed test of this model's validity in this case can be accomplished by fitting *individual vibronic transitions*, which are well-resolved in our higher resolution spectrum. The possibility of testing the accuracy of this numerical model by fitting individual transition position and intensity has not as far as we know been accomplished so far, and thus it may comprise a useful check on its validity. Finally, physical parameters such as shapes of the potential surface and the rate of electron transfer between subunits, as well as distortion energies and the strength of electronic coupling, can be analyzed within the context of this model.

PKS Method. The essence of the PKS method is to solve a set of secular equations that have been obtained through the use of a vibrational basis set of harmonic oscillator functions in a single coordinate q. The equations are not derived in this paper; most of the formulas are derived in ref 27–30.

The set of secular equations to be solved is

$$\sum_{n=0}^{\infty} r_{\nu n}(H_{mn} - \delta_{mn}E_\nu^+) = 0 \quad [m = 0, 1, 2, \ldots; \nu = 0, 1, 2, \ldots] \tag{11}$$

with

$$H_{mn} = \lambda[(m/2)^{1/2}\delta_{m,n+1} + ((m+1)/2)^{1/2}\delta_{m,n-1}] + \left(m + \frac{1}{2} + (-1)^m e\right)\delta_{m,n}$$

In these equations, the m, n, and ν are the indices of the orthonormal set of harmonic oscillator functions, E_ν^+ are the eigenvalues for the eigenfunctions

$$\Phi_\nu^+ = \Psi_+ \sum_{n=0,2,4}^{\infty} r_{\nu n}\chi_n + \Psi_- \sum_{n=1,3,5}^{\infty} r_{\nu n}\chi_n \tag{12}$$

where Ψ_+ and Ψ_- are the electronic wave functions and the χ_n are the vibrational wave functions which are the harmonic oscillator functions in coordinate q used as the vibrational basis set

$$\chi_{+,\nu} = \sum_{n=0}^{\infty} c_{\nu,n}\chi_n \qquad \chi_{-,\nu} = \sum_{n=0}^{\infty} c'_{\nu,n}\chi_n \tag{13}$$

The minus and plus subscripts indicate the vibronic and vibrational wave functions that do and do not change sign when the nuclei are interchanged.

The e is the electronic coupling parameter and is defined by

$$(h\nu_-)e \equiv (\Psi_a|V^{AB}|\Psi_b)^0 = \langle\Psi_a|H_{el}|\Psi_b\rangle^0 \tag{14}$$

and the λ is the vibronic coupling parameter defined by the relation

$$\lambda = (8\pi^2 h\nu_-^3)^{-1/2}l \tag{15}$$

where l defines the minimum in the totally symmetric normal coordinate Q by the equation for the vibrational potential energy W

$$W = W^0 + lQ + \tfrac{1}{2}kQ^2 \tag{16}$$

and $\nu_- = (2\pi)^{-1}(k)^{1/2}$ is the vibrational frequency of normal coordinate Q^-.

The infinite matrix corresponding to this set of secular equations is truncated and diagonalized. The basis size is simply increased to increase the numerical accuracy if necessary. The dipole strength of a vibronic line is evaluated by eq 17

$$D^e(\nu' \rightarrow \nu) = \left(\frac{N_{\nu'} - N_\nu}{N}\right)\delta_{\nu'\nu}{}^2|\langle\Psi_+|m_z^e|\Psi_-\rangle^0|^2 \tag{17}$$

with $\delta_{\nu'\nu} = \sum_n r'_{\nu'n}S_{\nu n}$, which are calculated from the coefficients of the vibronic eigenfunctions from the matrix diagonalization. In the transition dipole equation, the $N_{\nu'}/N$ is the fractional population in state ν' given by $\exp(-E_{\nu'}/kT)/\sum_\nu \exp(-E_{\nu'}/kT)$; m is the z component of the molecule-fixed electric dipole operator, $\vec{m} = \sum_i e_i\vec{r}_i$.

Application of PKS Theory to TQ_2^- Charge Resonance. In the case of the photodissociation spectrum of $(TQ)_2^-$, the low resolution data can be used to crudely define the parameters that can be used to fit the higher resolution data. First, the absolute cross section for photodissociation can be roughly estimated in order to get an estimate for the magnitude of e, because the cross section for absorption is highly sensitive to the electronic coupling parameter.

A number of assumptions are made in the estimate for the photodissociation cross section, all of which are reasonable. The trapping times for ions are assumed to be approximately 500 ms to 1 s, and the fractional signal decrease in approximately 20–25% at 500 mW incident laser power. If quantum yields are near unity, this results in a calculated absorption cross section of approximately 10^{-17} cm^2. By integrating the resonance through the frequency range with approximately this value of cross section, one can calculate that the vibronic overlap factors, $\sum_n r'_{\nu'n}S_{\nu n}$, cannot be significantly less than 0.01. With the summation of overlap factors on the order of this value, the electronic coupling parameter must be less than −6, and it should be greater than −9. This analysis assumes a value for the subunit separation of approximately 3.5 Å, in order to calculate the electronic contribution to the electronic dipole operator in eq 17.

A normal coordinate analysis of PBQ has been accomplished and gives rise to the lowest totally symmetric mode of 460 cm^{-1}. The frequency corresponding to this mode in TQ^- will be lower in frequency due to the heavy atom bonded to the ring. As a starting point for the spectral analysis, we chose 460 cm^{-1} as the active normal coordinate. The frequency is then adjusted as an additional parameter for a good fit to the data. With this value, I_{max} occurs at 33 to 34 quanta, and by using the determined range for e, a fit to the data results in a vibronic coupling parameter of $\lambda = 4.3$. This value of λ makes the width and spacings of the vibronic transitions relatively insensitive to e.

For these parameters of λ and e, which roughly give rise to the correct I_{max} and overall transition intensity, the theoretical spacings of the individual vibronic transitions are at 1.5 q (690 cm^{-1}). The normal coordinate frequency was then lowered to give the best fit to the data. The best fit was obtained at q = 300 cm^{-1}. For this frequency, the best overall fit to the resonance and the frequencies of the individual vibronic transitions is obtained with the parameters $e = -7$, $\lambda = 5.2$, and $T = 300$ K. Figure 6 is a result when synthesized Gaussian line shapes for each vibronic transition with half-widths of 0.66 q are used. Figure 7 displays the region in which the high resolution data were acquired, along with the experimental data. The transition energies are given in Table I, with the assignments showing the fit to the experimental data.

Interesting structural parameters of the dimer can be extracted from the fit if the parameters e and λ are reliable. The extent to which they are reliable will depend on the validity of the single oscillator model for a multi-oscillator dimer. The exact fitting of the vibronic transitions of the spectrum requires a lowering of the oscillator frequency from 460 to 300 cm^{-1}. This is a larger frequency shift than one might expect for a free ion complexing with a neutral molecule, but perhaps it is not out of range for an ion strongly interacting with the corresponding neutral molecule. The fit of six individual vibronic transitions in the observed spectrum strengthens the reliability of the parameters extracted,

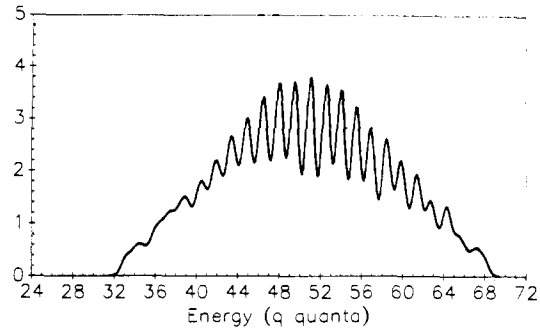

Figure 6. Theoretical charge resonance spectrum for $e = -7.0$, $\lambda = 5.2$, $q = 300$ cm^{-1}, $T = 300$ K.

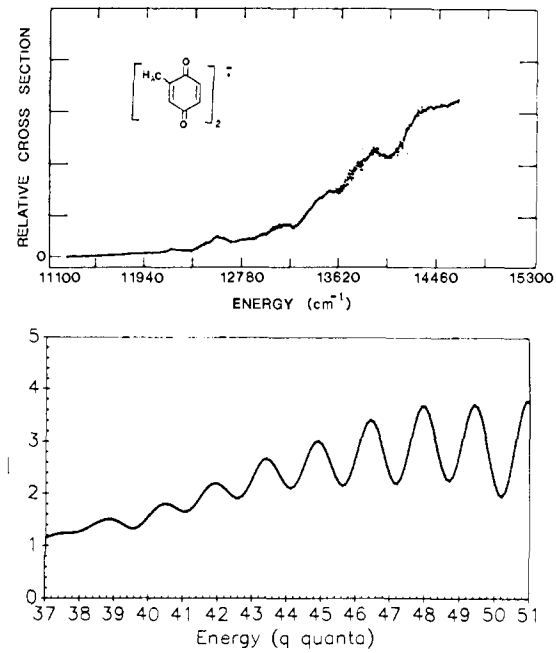

Figure 7. Lower panel: Detail of theoretical charge resonance spectrum as in Figure 6. Upper panel: Experimental spectrum in same region.

Table I. Calculated and Observed Transition Energies and Assignments for a Basis Set of 40 Quanta, with $q = 300$ cm^{-1} (the Ground and Excited Vibronic Manifold Is Denoted by v and v', Respectively)

obsd (cm^{-1})	calcd (cm^{-1})	quanta	assignments v'	assignments v
12180	12213	40.71	25-	2+
12560	12501	41.67	25-	1+
13060	12984	43.28	26+	1-
13520	13446	44.82	26-	1+
13920	13917	46.39	27+	1-
14350	14373	47.91	27-	1+

as opposed to fitting an overlapping overall band contour, as has been done previously in the near-IR spectral region.

A quantitative description of the degree of delocalization in the quinone dimer ion is given by examining the integration of the vibronic wave functions over the vibrational coordinate q:

$$P_v(\mathrm{el}) \equiv \int |\Phi_v|^2 \, dq = \frac{1}{2}(\Psi_a^2 + \Psi_b^2) + (\Psi_a^2 - \Psi_b^2)\sum_{n=0}^{\infty} r_{vn}r'_{vn} + \Psi_a\Psi_b\sum_{n=0}^{\infty}(r_{vn}^2 - r'^2_{vn}) \quad (18)$$

For the symmetrical dimer, the + functions are

$$P_v^+(\mathrm{el}) = \frac{1}{2}(\Psi_a^2 + \Psi_b^2) + \Psi_a\Psi_b\left(\sum_{n=0,2,4}^{\infty} r_{vn}^2 - \sum_{n=1,3,5}^{\infty} r_{vn}^2\right) \quad (19)$$

The degree of delocalization of the excess electron within the symmetric dimer is given by the square of the $\Psi_a\Psi_b$ coefficient. The $\Psi_a^2 = |\Psi_M^A\Psi_N^B|^2$ represents the probability of simultaneously finding center A in oxidation state M and center B in oxidation state N, and $\Psi_b^2 = |\Psi_N^A\Psi_M|^2$ represents the reverse. If several states are thermally populated, the thermal average of the coefficient is calculated and is given by

$$\bar{\beta}_d^2 = \sum_v \exp(-E_v/kT)\left[\sum_{n=0,2,4}^{\infty} r_{vn}^2 - \sum_{n=1,3,5}^{\infty} r_{vn}^2\right]^2 / \sum_v \exp(-E_v/kT) \quad (20)$$

For the region of parameter space of interest, the degree of delocalization was calculated and is displayed in Figure 8. One can see that the extent of delocalization is between 5 and 10% for $e = -6$, -7, -8 and $\lambda = 5.2$. We conclude from the observed spectral fit that this model represents the dimer as a "solvated" localized anion and not a delocalized dimer ion.

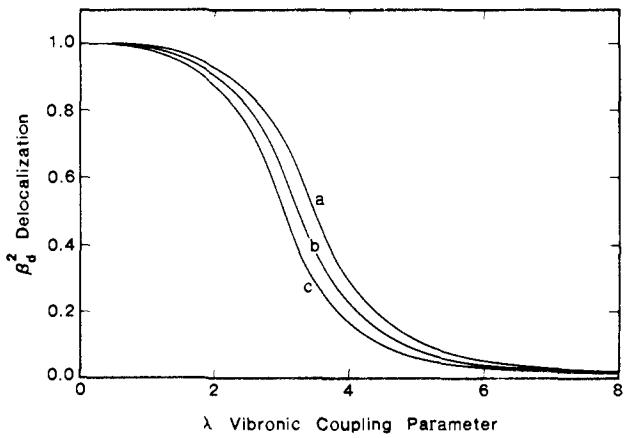

Figure 8. Degree of delocalization as a function of vibronic coupling, for $e = -6$, -7, and -8 (lines a, b, and c, respectively).

The preceding vibronic coupling analysis of the charge resonance transition attributes the vibronic transition locations as being due to a frequency dispersion between the coupled states. There are, however, three terms that contribute to the second central moment μ_2 of an absorption envelope.[32] In Hush's notation these are

$$\mu_2 = \mu_2(\Delta) + \mu_2(\Gamma) + \mu_2(\mathrm{LW}) \quad (21)$$

The first term is the contribution from the displacement from equilibrium positions in the upper and lower states. The second results from frequency dispersion and is a function of the difference in force constants of the upper and lower surfaces. The last term is the line width of the individual vibronic transition.

As has been pointed out by Hush,[32] in the vibronic analysis of PKS the bandwidth results from the frequency dispersion plus a contribution from the line width. For a delocalized system, the bandwidth is then predicted to be narrow, with only a few vibronic transitions contributing to the line shape.

If the system is delocalized the optical excitation is of the type $\Psi_{\mathrm{bonding}} \rightarrow \Psi_{\mathrm{antibonding}}$, and a change in bond length would occur. In this case the distance dispersion term would be an important contributor to the overall line shape. This would result in a progression in single quanta of a totally symmetric mode. If this strongly features in the line shape, as it could in a delocalized case, then the PKS model may be inappropriate for the spectral analysis.

Conclusions

The charge resonance spectrum of the negative ion dimer of *p*-toluquinone has been experimentally determined in the gas phase by photodissociation spectroscopy. At low resolution, a charge resonance band was located and is at substantially lower energies than the transitions due to an isolated toluquinone molecule or negative ion. At higher resolution, vibronic structure of the charge resonance is clearly identified. The transitions were calculated with PKS theory and were fit to reasonable accuracy considering

(32) Hush, N. S. *NATO Adv. Study Inst. Ser., Ser. C* **1980**, *58*, 151-181.

the simplicity of the model. The energies involved in the interaction of the molecule and ion were elucidated, and the degree of delocalization of the excess electron was calculated. The PKS analysis indicates the ion is strongly localized and would be best described as a "solvated" ion. An alternative description of the excitation which includes a distance dispersion would describe the dimer ion as being delocalized.

Acknowledgement is made to the National Science Foundation for support of this research and to the donors of the Petroleum Research Fund, administered by the American Chemical Society. We thank Professor Noel Hush for many useful suggestions regarding the interpretation of the charge resonance spectrum.

Registry No. $(TQ)_2^{\bullet-}$, 110850-67-4; quinhydrone, 106-34-3.

Ion/Surface Interactions as a Tool for Characterizing Isomers: $[C_2H_4O]^{\bullet+}$ Ions

Md. A. Mabud, T. Ast,† S. Verma, Y.-X. Jiang, and R. G. Cooks*

Contribution from the Department of Chemistry, Purdue University, West Lafayette, Indiana 47907. *Received November 28, 1986*

Abstract: Mass-selected $[C_2H_4O]^{\bullet+}$ ions, subjected to low-energy (25–60 eV) collisions at a solid surface, undergo inelastic scattering leading to surface-induced dissociation (SID) in competition with hydrogen atom abstraction. The spectra of isomeric ions show more pronounced differences than observed in gas-phase collision-activated dissociation (CAD). Control of the energy transferred to the selected ion is achieved by control of the collision energy in low-energy gas-phase and surface collisions and by selection of the scattering angle (0–5° lab) in high-energy gas-phase collisions. The SID and CAD data agree well and confirm the structures of the $[C_2H_4O]^{\bullet+}$ ions generated from acetaldehyde and butyraldehyde as the ketonic and enolic species a and b, that from ethylene carbonate as d, and that from pyruvic acid as the ionized carbene f. The ions derived from both ethylene oxide and ethylene carbonate behave indistinguishably to those derived from ethylene oxide in CAD and SID, indicating that they have the same structure or mixture of structures. While the cyclic ion c is not excluded, ring opening of ethylene oxide is argued to occur and to take place by C–C rather than by C–O bond cleavage, giving structure d rather than e as the major $[C_2H_4O]^+$ ion derived from ethylene oxide, ethylene carbonate, and 1,3-dioxolane. Either prior to or, more probably, upon activation, rearrangement occurs to give the ionized carbene f and the ylide g. Both of these ions have free methyl groups which are readily recognized upon collisional activation. The new methods used here clarify ion structural questions regarding the $[C_2H_4O]^+$ ion and provide the first experimental evidence for the participation of the isomer g.

The problem of characterizing the structures of gaseous organic ions has drawn upon a range of techniques,[1] including ion/molecule reactions,[2] collisional activation,[3] metastable ion dissociations,[4] and charge stripping.[5] Neutralization–reionization sequences[6] are a recent addition to this list.

Polyatomic ion/surface collisions provide a means of characterizing ions through their dissociation products.[7] Daughter spectra of selected ions can be obtained after inelastic collisions, the internally excited ions fragmenting in the gas phase by a process referred to as surface-induced dissociation (SID). The amount of internal energy deposited in the activated ion can be controlled by selection of the collision energy.[7,8] This method allows higher average energy deposition than does gas-phase collisional activation in either the low (eV) or high (keV) range of collision energies,[7] a result that may prove significant in the mass spectrometry of large molecules which are difficult to dissociate.[9] Parent, neutral loss, charge exchange, and reflection spectra, additional ways of accessing the data domain of tandem mass spectrometry, are also available through ion/surface interactions.[10,11]

In the course of studies of ion/surface collision phenomena, we have observed that certain ions pick up a hydrogen atom(s) or a methyl group upon colliding with the (gas-covered) surface. Reactive collisions of organic ions at solid surfaces have not previously been reported. The nature of this and related reactive collisions is currently being systematically studied, and the results will be reported elsewhere. In the present investigation we employ daughter spectra that include ions resulting from both ion/surface reactive collisions as well as surface-induced dissociation, to distinguish between isomeric ions.

Chart I

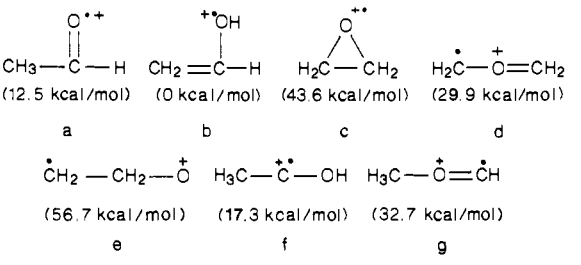

Both as a test of the capabilities of the SID method and for its intrinsic importance, we have chosen a classic problem in ion structure, that of the isomeric $[C_2H_4O]^{\bullet+}$ ions. Calculations have

† Department of Technology and Metallurgy, University of Belgrade, Belgrade, Yugoslavia.

(1) (a) Holmes, J. L. *Org. Mass Spectrom.* **1985**, *20*, 169. (b) Levsen, K. *Fundamental Aspects of Organic Mass Spectrometry*; Verlag Chemie: Weinheim, New York, 1978.
(2) (a) Bowers, M. T., Ed. *Gas Phase Ion Chemistry*; Academic: New York, 1979; Vol. 1. (b) Gross, M. L.; Russell, D. H.; Aerni, R. J.; Broncyzk, S. A. *J. Am. Chem. Soc.* **1977**, *99*, 3603.
(3) Levsen, K.; Schwarz, H. *Mass Spectrom. Rev.* **1983**, *2*, 77.
(4) Holmes, J. L.; Terlouw, J. K. *Org. Mass Spectrom.* **1980**, *15*, 383.
(5) Ast, T. In *Advances in Mass Spectrometry*; Todd, J. F. J., Ed.; John Wiley and Sons: New York, 1986; in press.
(6) Danis, P. O.; Wesdemiotis, C.; McLafferty, F. W. *J. Am. Chem. Soc.* **1983**, *105*, 7454.
(7) Mabud, Md. A.; DeKrey, M. J.; Cooks, R. G. *Int. J. Mass Spectrom. Ion Proc.* **1985**, *67*, 285.
(8) DeKrey, M. J.; Kenttämaa, H. I.; Wysocki, V. H.; Cooks, R. G. *Org. Mass Spectrom.* **1986**, *21*, 193.
(9) Neumann, G. M.; Derrick, P. J. *Org. Mass Spectrom.* **1984**, *19*, 165.
(10) DeKrey, M. J.; Mabud, Md. A.; Cooks, R. G.; Syka, J. E. P. *Int. J. Mass Spectrom. Ion Proc.* **1985**, *67*, 295.
(11) Mabud, Md. A.; DeKrey, M. J.; Cooks, R. G.; Ast, T. *Int. J. Mass Spectrom. Ion Proc.* **1986**, *69*, 277.

0002-7863/87/1509-7597$01.50/0